DOI 10.1007/s10527-020-09998-y
Biomedical Engineering, Vol. 54, No. 3, September, 2020, pp. 174-178. Translated from Meditsinskaya Tekhnika, Vol. 54, No. 3, May-Jun., 2020, pp. 14-17.
Original article submitted July 1, 2019.

Detection of Microcalcifications Using the Ultrasound Doppler Twinkling Artifact

D. V. Leonov[1,2]*, N. S. Kulberg[1], A. I. Gromov[3], and S. P. Morozov[1]

We analyzed the possibility to detect microcalcifications using a novel ultrasound diagnostic mode based on advanced analysis of the color Doppler twinkling artifact. The special mode was tested with two phantoms: a commercially available polyurethane mammographic breast phantom with dense inclusions simulating microcalcifications and a phantom developed in our laboratory and containing chemically grown $CaSO_4$ microcrystals less than 200 μm in size. The mineral inclusions in the first phantom were visible in B-mode and correctly detected with the novel mode. The presence of inclusions in the second phantom was not obvious when imaged in B-mode; however, it was reliably detected with the special mode. The special mode used two colors to distinguish between the physical processes behind the color Doppler twinkling artifact — elastic vibration and microcavitation. This research demonstrated the applicability and usefulness of the special diagnostic mode for the detection of microcalcifications in phantoms.

Introduction

Detecting breast cancer at an early stage remains a key problem, whose solution would significantly reduce female mortality worldwide. Microcalcifications are an important, and sometimes the only, diagnosed symptom of early breast cancer not yet detectable by palpation [1-5].

Computed tomography (CT), X-ray mammography, and ultrasound examination are used to detect microcalcifications. Ultrasound has such well-known advantages as mobility, availability, relatively low cost of the examination, absence of harmful radiation, and, in some cases, portability. Ultrasound is a primary means of needle guidance during a biopsy. However, the diagnostic efficiency of ultrasound for detecting microcalcifications is significantly lower than that of computed tomography.

Attempts were made to increase the diagnostic efficiency through the development of specialized mammographic ultrasound scanners [5] operating at frequencies of 13 MHz and higher to provide high scanning resolution. The results of diagnostics with such scanners are less operator-dependent because of the use of special sensors and three-dimensional scanning. The use of diagnostic modes specifically designed to detect mineral inclusions is also known to improve the accuracy of ultrasound machines [6-12]. One such mode was developed by our team. It is based on the analysis of the twinkling artifact – a phenomenon that manifests itself in Doppler modes and has been proven useful in the diagnosis of calculi [13-20].

The goal of this work was to analyze the possibility of ultrasound detection of microcalcifications with the special mode developed by our team on the basis of the analysis of the underlying mechanisms [9, 11] of the Doppler twinkling artifact.

Materials and Methods

The study was carried out using a Sonomed-500 diagnostic ultrasound device (Spectromed, Moscow). The device software offers a special operation mode developed by our team at the Research and Practical Clinical Center for Diagnostics and Telemedicine

[1] Research and Practical Clinical Center for Diagnostics and Telemedicine Technologies of the Moscow Health Care Department, Moscow, Russia; E-mail: d.leonov@npcmr.ru
[2] National Research University "Moscow Power Engineering Institute", Moscow, Russia.
[3] A. I. Evdokimov Moscow State University of Medicine and Dentistry, Moscow, Russia.
* To whom correspondence should be addressed.

Technologies of the Moscow Health Care Department and intended to detect solid mineral inclusions [9-12], i.e., objects with densities significantly different from those of the surrounding tissues and fluids; for example, microcalcifications, calcifications, kidney and bladder stones, etc.

The special diagnostic mode is based on the analysis of the received radio-frequency signals [6]. Preliminary tests involved the detection of solid objects larger than 1.5 mm in size [11]. The ultrasound device operates in duplex mode, i.e., a map of the distribution of mineral inclusions is superimposed on a gray-scale echogram. Two colors are used for mapping to indicate the difference in the nature and characteristics of the recorded signals [10]. Turquoise is used to indicate microcavitation signals, while yellow highlights elastic microvibrations (motion) of the object. According to [12], microcavitation leads to type 1 artifact; microvibrations, to type 2 artifact. These are two types of the twinkling artifact. This artifact appears in Doppler modes in hyperechoic objects and is used for their detection [13-20].

Small mineral inclusions were the object of this study. First, a Blue Phantom BP1901 polyurethane mammographic phantom was used in the tests (Figs. 1 and 2). The dimensions of the breast phantom were 170 × 120 × 45 mm. The phantom contained artificial heterogeneities, some of which simulated microcalcifications. The characteristics of the artificial inhomogeneities used in the phantom can be found in [21]. The object under study with simulated microcalcifications was 15 mm in diameter. The Young's modulus of the object was measured by shear wave elastography and found to be in the range of 100-140 kPa.

Then, $CaSO_4$ microcrystals grown chemically from CaCl and $CuSO_4$ in agar jelly were studied (Fig. 3 and 4). The size of the crystals was up to 200 μm (Fig. 3a), which is approximately the size of microcalcifications observed by mammography [3]. The density of the crystals was approximately 2.3 g/cm^3. We also used a control sample that did not contain microcrystals (Fig. 3b). Both samples were placed 20 mm deep on a sound-absorbing substrate and immersed in water.

All experiments were carried out using a 7.5L37 linear transducer in duplex mode. Imaging in B-mode was performed at 9.4 MHz; in the Doppler mode with a pulse repetition rate of 500 Hz, at 6.3 MHz.

Results and Discussion

Figure 1 shows a CT image of the mammographic phantom. This phantom incorporated various simulated

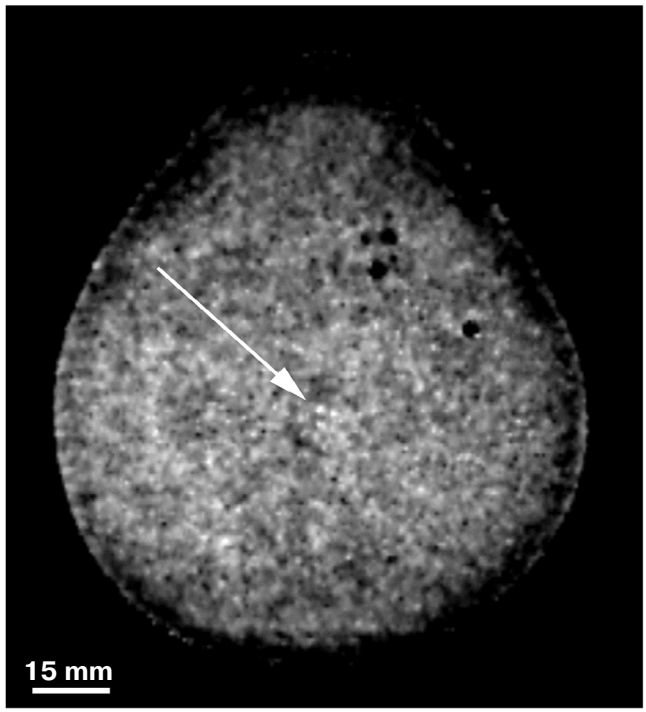

Fig. 1. CT image of the breast phantom (microcalcifications are indicated with an arrow).

tumors, some of which contained mineral inclusions similar in properties to microcalcifications. These simulated tumors were visible in B-mode (Fig. 2a). In the color flow mapping mode with a standard breast examination preset, the twinkling artifact did not appear. When imaged in the special visualization mode, all these objects were highlighted in yellow to indicate that the machine registered the motion or microvibration of the scatterers (type 2 artifact; Fig. 2b). This is an expected result because the nucleation of microbubbles through cavitation requires the presence of a liquid, which is absent in the polyurethane phantom.

A method for detecting microcalcifications by recording elastic vibrations is also described in [7, 8]. However, this method requires additional pushing pulses hundreds of microseconds long, while the mode considered in this work uses standard Doppler signals [9].

Figure 3 shows images of the sample with microcalcifications (a) and the control sample (b). As they grew, microcrystals formed clusters on the surface of the material. Inside the tissue-simulating material, there were fewer crystals and they were smaller in size. However, it is these crystals that are of the greatest interest. That is why we used for ultrasound examination relatively thin samples cut from the bulk of the tissue-simulating material,

where the microcalcifications were the smallest. The enlarged photograph in Fig. 3a shows that the microcalcifications did not exceed 200 μm in size.

Figure 4 shows ultrasound images of the sample with microcalcifications (left) and the control sample (right). It can be seen from Fig. 4a that in B-mode the two samples have similar echogenicity. In Fig. 4b, the B-image is overlaid with the map obtained in the mode under consideration. The map shows the surface areas of the sample with microcalcifications highlighted in two colors. This means that both types of signals were detected, i.e., not only elastic vibrations, as in the polyurethane phantom (Fig. 2b), but microcavitation signals (type 1 artifact [11]) as well.

It is of special interest that the developed mode allowed the detection of microcalcifications (Fig. 4b). Visualizing such microcalcifications with conventional ultrasound techniques is challenging due to the small size and the absence of acoustic shadows. Rather than being completely reflected, as in the case of large kidney stones,

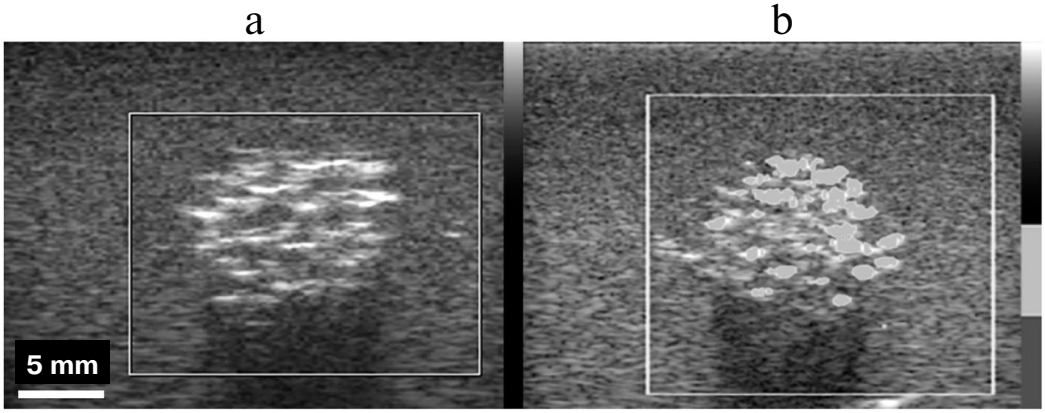

Fig. 2. Echograms of calcifications in the breast phantom: a) mineral inclusions are visible in B-mode; b) the mode for detecting mineral inclusions highlights them in color.

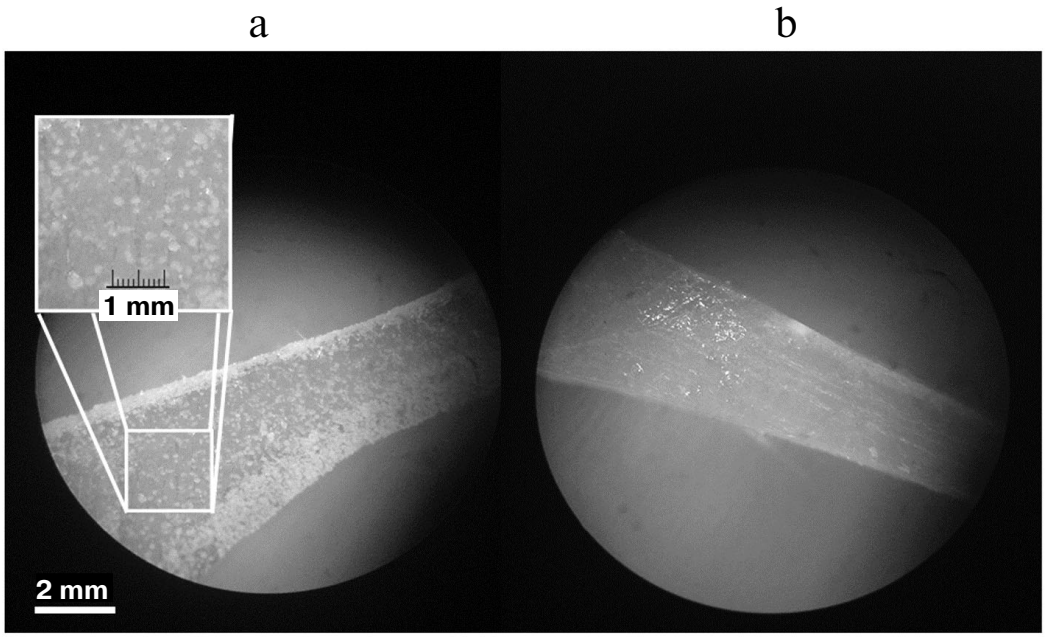

Fig. 3. Microphotographs: a) sample with microcalcifications 200 μm in size; b) control sample without microcalcifications.

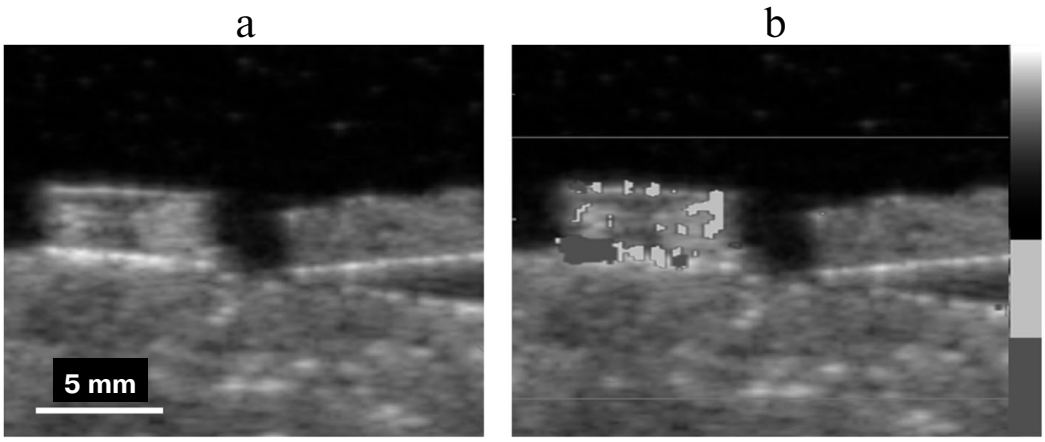

Fig. 4. Echogram: a) the gray-scale mode does not allow unequivocal detection of microcalcifications; b) the mode for detecting mineral inclusions highlights certain regions inside the sample with microcalcifications. There are no highlighted regions in the control (microcalcification-free) sample.

the ultrasound wave incident on such microcalcifications is for the most part scattered, which makes detection difficult. In contrast to B-mode, the mode under consideration uses Doppler signals, which are sensitive to phase changes. Phase methods are more effective than amplitude methods for detection purposes because they can provide additional information about the signal [6]. As a result, the mode under consideration makes it possible to detect dense objects that are indistinguishable to conventional ultrasound techniques. Such objects do not produce ultrasound shadows and do not stand out in brightness against the surrounding tissues.

Conclusions

A special diagnostic mode for detecting calculi in ultrasound images was studied. The mode had been developed by our team and previously tested in various relatively large objects (more than 1.5 mm in size) [10, 11]. Similar to color flow mapping, which creates a map of blood vessels, our mode builds a map of mineral inclusions. The obtained maps are superimposed on B-images. The mapping utilizes a two-color scheme to indicate the difference in the nature and characteristics between the echoes from mineral inclusions.

In this paper, microcrystals grown in agar jelly and a breast phantom with small mineral inclusions were used as test objects. The study showed that the developed mode can detect microcalcifications less than 200 μm in size. However, as the study was conducted only in phantoms, further clinical trials are needed to evaluate the applicability of the developed diagnostic mode in mammography patients.

This work was supported by the Russian Foundation for Basic Research (Grant No. 17-01-00601).

REFERENCES

1. Hellgren, R., Dickman, P., Leifland, K., Saracco, A., Hall, P., and Celebioglu, F., "Comparison of handheld ultrasound and automated breast ultrasound in women recalled after mammography screening," Acta Radiol., **58**, No. 5, 515-520 (2016).
2. Abduramov, A. B., "CT-mammography with intravenous contrast in the diagnosis of recurrent breast cancer," Russ. Electron. J. Radiol., **1**, No. 1, 17-25 (2011).
3. Chen, P. H., Ghosh, E. T., Slanetz, P. J., and Eisenberg, R. L., "Segmental Breast Calcifications," Amer. J. Roentgenol., **199**, No. 5, W532-W542 (2012).
4. Lesko, K. A., Matkhev, S., Abduraimov, A. B., and Boiko, E. A., "Current state of mammographic screening for breast cancer," Russ. Electron. J. Radiol., **2**, No. 3, 77-82 (2012).
5. Stoblen, F., Landt, S., Ishaq, R., Stelkens-Gebhardt, R., Rezai, M., Skaane, P., Blohmer, J. U., Sehouli, J., and Kummel, S., "High-frequency Breast Ultrasound for the Detection of Microcalcifications and Associated Masses in BI-RADS 4a Patients," Anticancer Res., **31**, No. 8, 2575-2581 (2011).
6. Leonov, D. V., Kulberg, N. S., Fin, V. A., and Gromov, A. I., Method for Detecting Physical Density Anomalies in Acoustic Imaging, RF Patent No. 2665223 (2017).
7. Andreev, V. G., Shanin, A. V., and Demin, I. Yu., "Motion of a group of microparticles in a viscoelastic medium under the action of acoustic radiation force," Acoust. Phys., **60**, No. 6, 704-709 (2014).
8. Andreev, V. G., Demin, I. Yu., Korolkov, Z. A., and Shanin, A. V., "Motion of spherical microparticles in a viscoelastic medium under the action of acoustic radiation force," Bulletin of the Russian Academy of Sciences: Physics, **80**, No. 10, 1191-1196 (2016).

9. Leonov, D. V., Kulberg, N. S., Gromov, A. I., Morozov, S. P., and Kim, S. Yu., "Causes of ultrasound Doppler twinkling artifact," Acoust. Phys., **64**, No. 1, 105-114 (2018).
10. Kulberg, N. S. and Leonov, D. V., Ultrasonic Mineral Inclusions Detector, Software Certificate RUS 2018610936 (2017).
11. Leonov, D. V., Kulberg, N. S., Gromov, A. I., Morozov S. P., and Vladzimirskiy, A. V., "Diagnostic mode detecting solid mineral inclusions in medical ultrasound imaging," Acoust. Phys., **64,** No. 5, 624-636 (2018).
12. Kulberg, N. S., Gromov, A. I., Leonov, D. V., Osipov, L. V., Usanov, M. S., Morozov, S. P., and Vladzimirskii, A. V., "Ultrasound diagnostic mode for kidney stone and soft tissue calculi detection," Radiol. Prakt., **67**, No. 1, 37-49 (2018).
13. Gromov, A. I. and Kubova, S. Yu., Ultrasonic Artifacts [in Russian], Vidar, Moscow (2007).
14. Aytac, S. K. and Ozcan, H., "Effect of color Doppler system on the "twinkling" sign associated with urinary tract calculi," J. Clin. Ultrasound, **27**, No. 8, 433-439 (1999).
15. Behnam, H., Hakkam, A., and Rakhshan, H., "Modeling twinkling artifact in sonography," in: 4th Int. Conf. Bioinformatics and Biomedical Engineering (2010).
16. Denstedt, J. and Rosette, J., International Consultation on Urological Diseases. Stone Diseases, Société Internationale d'Urologie, Glasgow (2014).
17. Gao, J., Hentel, K., and Rubin, J. M., "Correlation between twinkling artifact and color Doppler carrier frequency: Preliminary observations in renal calculi," J. Ultrasound Med. Biol., No. 9, 1534-1539 (2012).
18. Hirsch, M. S., Palavencino, T. B., and Leon, B. R., "Color Doppler twinkling artifact: A misunderstood and useful sign," Revista Chilena de Radiol., **17**, No. 2, 82-84 (2011).
19. Wang, M., Li J., Xiao, J., Shi, D., and Zhang, K., "Systematic analysis of factors related to display of the twinkling artifact by a phantom," J. Ultrasound Med., **30**, No. 11, 1449-1457 (2011).
20. Weinstein, S. P., Seghal, C., Conant, E. F., and Patton, J. A., "Microcalcifications in breast tissue phantoms visualized with acoustic resonance coupled with power Doppler US: Initial Observations," Radiology, **224**, No. 1, 265-269 (2002).
21. Kulberg, N. S., Osipov, L. V., and Usanov, M. S., "Comparative analysis of ultrasound elastography technologies and the use of an elastographic phantom," Radiol.-Prakt., **56**, No. 2, 6-23 (2016).